

DeepSPF: Spherical SO(3)-Equivariant Patches for Scan-to-CAD Estimation

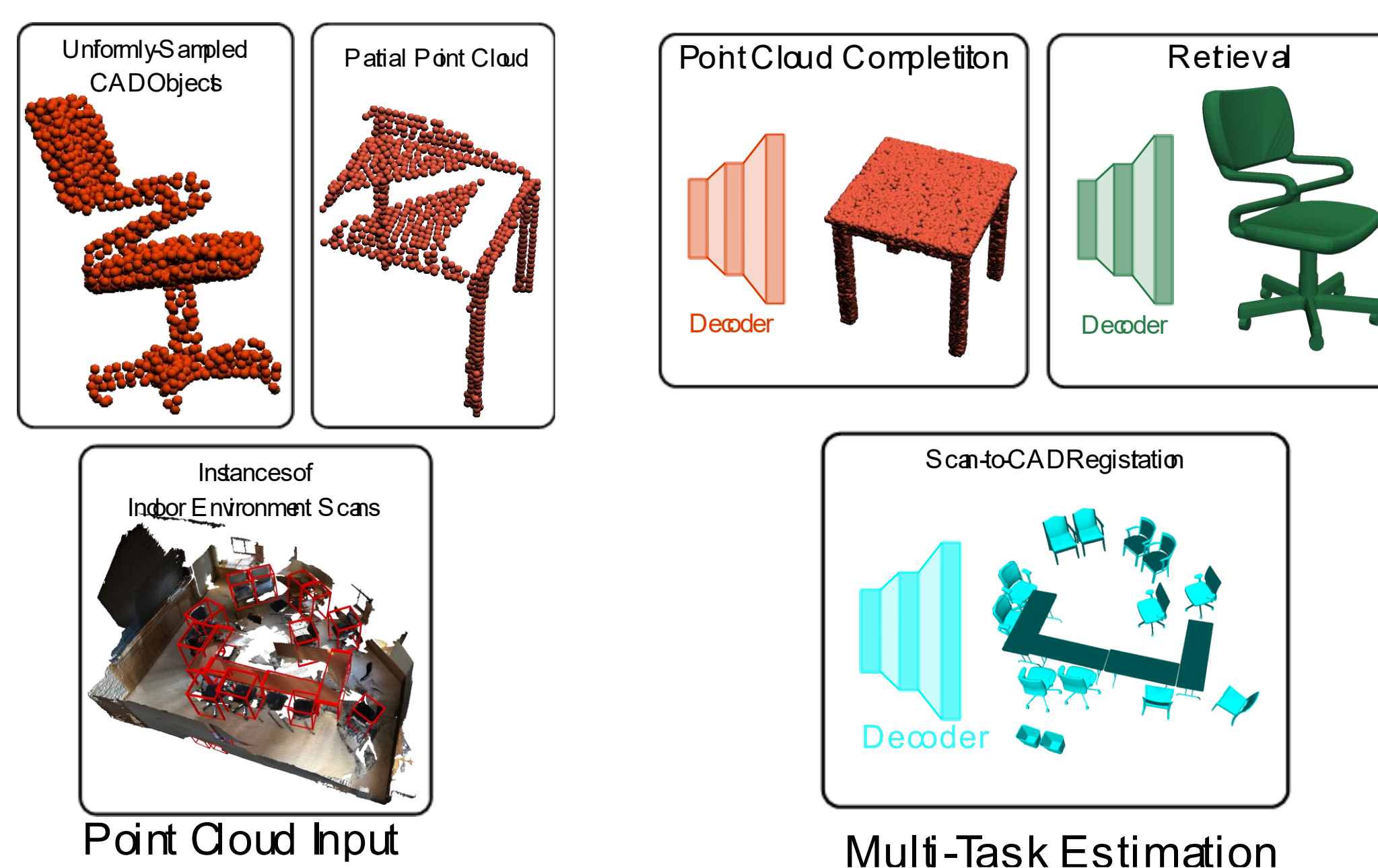
Driton Salihu¹, Adam Misik^{1,2}, Yuankai Wu¹, Constantin Patsch¹, Fabian Seguel¹, Eckehard Steinbach¹

¹ Technical University of Munich
School of Computation, Information and Technology,
Department of Computer Engineering, Chair of Media Technology,
Munich Institute of Robotics and Machine Intelligence (MIRMI)
²Siemens Technology

Information

We introduce Spherical Patch Fields, a representation technique designed for patch-wise, SO(3)-equivariant 3D point clouds, anchored theoretically on the principles of Spherical Gaussians. Second, we present the Patch Gaussian Layer, designed for the adaptive extraction of local and global contextual information from resizable point cloud patches. Culminating our contributions, we present Learnable Spherical Patch Fields (DeepSPF) – a versatile and easily integrable backbone suitable for instance-based point networks.

Motivation

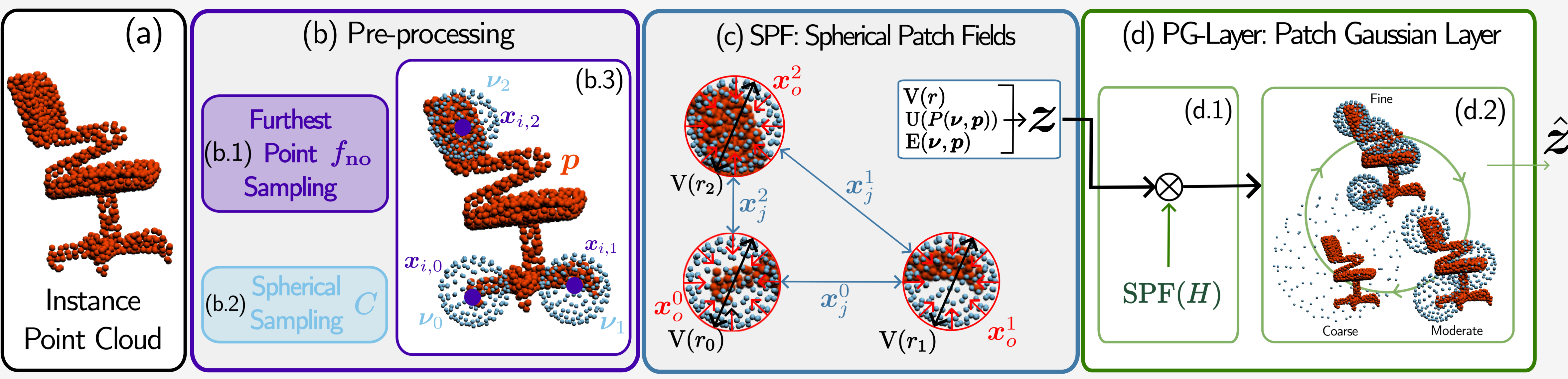


Problems:

- Registration:** Uniformly sampled CAD object and scanned object have no point-to-point correspondences
- Retrieval:**
 - CAD object and scanned object have no point-to-point correspondences
 - Pose and scale are vastly different between sensor and designed object
 - Overall similar structures but patch-wise differences
- Completion:** Vast amount of augmentation needed Learning different over different datasets

Approach

DeepSPF: Learnable Spherical Patch Fields



$$\text{SPF}(\mathbf{p}; \lambda, \boldsymbol{\nu}, r) = \mathbf{E}(\boldsymbol{\nu}, \mathbf{p}) \mathbf{V}(r) \mathbf{U}(P(\boldsymbol{\nu}, \mathbf{p})) e^{\lambda(\boldsymbol{\nu}^T \mathbf{p} - 1)}$$

Spatial Graph | Volume Information | Low frequency information

We present a network that represents a point cloud through a patch-wise rotation-equivariant radial representation termed SPF. PG-Layer improves the learnable SPF representation using low-frequency information and adaptive resizable patches.

Quantitative Evaluation

Model	$d_C \downarrow$	RRMSE \downarrow	RMSE(t) \downarrow	Model	$d_C \downarrow$	RRMSE \downarrow	RMSE(t) \downarrow
DCP (Wang & Solomon, 2019)	0.059	93.221	0.014	PointNetLK (Aoki et al., 2019)	0.026	81.843	1.037
RGM (Fu et al., 2021)	0.254	100.97	0.388	DCP (Wang & Solomon, 2019)	0.055	90.715	0.014
RoTr (Yu et al., 2023)	-	81.14	0.1353	RGM (Fu et al., 2021)	0.254	100.11	0.389
DeepGMR (Yuan et al., 2020)	0.026	67.282	0.010	DeepGMR (Yuan et al., 2020)	0.011	42.515	0.004
DeepUME (Lang & Francos, 2021)	0.011	70.818	0.009	DeepUME (Lang & Francos, 2021)	0.002	2.425	0.001
SGPCR (Salihu & Steinbach, 2023)	0.0010	8.57	0.0034				
Ours (E)	0.0007	7.45	0.0031	Ours + DeepGMR (Yuan et al., 2020)	0.0001	0.40	0.0068
Ours (E+U)	0.0006	6.49	0.0029				
Ours (E+U+V)	0.0004	5.17	0.0022				
Ours + DeepGMR (Yuan et al., 2020)	0.0016	5.32	0.0210				

We demonstrate significant enhancements in Scan-to-CAD performance for point cloud registration, retrieval, and completion.

Class	Avetisyan et al. (2019a)	Avetisyan et al. (2019b)	Avetisyan et al. (2020)	Ours
Bathtub	36.20	38.89	42.42	56.66
Cabinet	34.00	51.52	58.33	56.22
Chair	44.26	73.04	81.23	78.39
Sofa	30.66	76.92	82.86	73.56
Table	30.11	48.15	45.60	61.64
Bin	20.60	18.18	32.26	36.99
Avg. \uparrow	38.17	51.11	57.11	60.57

Qualitative Evaluation

